Research Square

Preprints are preliminary reports that have not undergone peer review.
They should not be considered conclusive, used to inform clinical practice,
or referenced by the media as validated information.

Examining the Effects of Post Weld Heat Treatment on the Microstructure and Mechanical Properties of Friction Stir Welded Low Carbon Steel

MOHAMED FAYAS SAFFIUDEEN

mfsaffiudeen@lincoln.edu.my

Lincoln University College https://orcid.org/0000-0003-0977-6166

Mohammad Nizamuddin Inamdar

Lincoln University College

Research Article

Keywords: SA516 Grade 70, Friction Stir Welding, PWHT, Hardness, Tensile

Posted Date: September 29th, 2026

DOI: https://doi.org/10.21203/rs.3.rs-10813857/v1

License: This work is licensed under a Creative Commons Attribution 4.0 International License.
Read Full License

Examining the Effects of Post Weld Heat Treatment on the Microstructure and Mechanical Properties of Friction Stir Welded Low Carbon Steel

Mohamed Fayas Saffiudeen [1], Dr. Mohammad Nizamuddin Inamdar[2]
Research Scholar [1], Associate Professor [2], Faculty of Engineering and Built Environment,
Lincoln University College, Selangor,Malaysia.
Correspondence email: mfsaffiudeen@lincoln.edu.my; nizamuddin@lincoln.edu.my

Abstract

This study investigates the effect of friction stir welding and PWHT on the mechanical properties of low carbon steel. Parameters of FSW studied include tool diameters of 4, 5, and 6 mm; welding speeds of 40, 55, and 70 mm/min; and tool rotation speeds of 1000, 1100, and 1200 RPM. These parameters were optimized using the L9 orthogonal array, which also served in studying their effect on weld performance. Optimal parameters recognized were tool rotation speed 1100 RPM, welding speed 40 mm/min, and tool pin diameter 5 mm. Welding speeds beyond 70 mm/min and rotation speeds of 1200 RPM adversely affected mechanical properties, probably due to either poor consolidation of material or excessive heat input. Tensile strength declined from 540 N before PWHT to 523 N after PWHT, with hardness falling from 188 HV to 179 HV, thereby indicating that PWHT softened the weld while releasing residual stresses. In microstructural analysis, PWHT caused an increase of ferrite and spheroidized pearlite, which brought a slight decrease in strength and hardness but a remarkable increase in impact toughness and ductility. This study contributes insight to effectively optimize the parameters of FSW in industrial applications while ensuring a reliable compromise between strength, hardness, and overall weld integrity.

Keyword: SA516 Grade 70; Friction Stir Welding; PWHT; Hardness; Tensile;

1.Introduction

FSW was introduced as a novel welding process by TWI in 1991. From its inception, FSW has attracted great interest especially in applications for low melting point materials such as copper, magnesium and aluminum alloys. However, an appropriate tool material could not be found that could withstand the extreme temperature of over 1000 °C, thus limiting the application of FSW with steel and other high temperature materials [2-14]. Stainless and alloy steels are used in very minimal amounts in the oil and gas sectors while building pipes, heat exchangers, pressure vessels, fin fan coolers, and boilers using carbon steel is the main priority [15-20]. These welding techniques are currently the most used in construction and maintenance of oil and gas infrastructures, owing to their reputation with regard to reliability and adaptability for joining a variety of materials: GTAW and SMAW. The most notable feature of GTAW welding is the fact that it produces very precise and clean welds, which are often highly sought in applications where every detail is counted on to be accurate. However,

SMAW is preferred because it is easy to understand and very effective in maintenance environments [21-28]. In addition, gas metal arc welding has become notorious for speed and ease of use in new fabrication schemes. While submerged arc welding produces strong welds and high rates of deposition, it is limited in applications to ones in plants because of accessibility issues because its set up needs particular arrangements that might not be possible in small areas. Furthermore, FSW has not been used extensively in this field, more especially regarding SA 516 Gr. 70, a material that is typically used in the oil and gas industry specially for heat exchangers, pressure vessels, reboilers, condensers, finfan coolers. The major constraint behind this restriction is the unavailability of optimized process parameters specifically for this material. Though the FSW technique has a significant potential, still further refinement is needed to its parameters for diverse applications. [29-36].

Despite the remarkable advancements in FSW for carbon steels, the establishment of effective and optimal process parameters for the SA 516 Gr. 70 N low carbon steel plates, idle or in a PWHT condition, is still the focus of intensive research. These two necessities require innovative ways of selecting the process parameters, given that carbon steel welding has high thermal and mechanical demand. The thrust for developing new coatings and materials is to improve the performance and life of FSW in hostile environments. These advances may open up new applications for FSW beyond its conventional uses by providing a promising welding technique suitable for a wider range of engineering materials with and without PWHT. This is all the more relevant for modern day manufacturing and structural applications across various industries, such as nuclear, automotive, aerospace, thermal power plants, petrochemical processes, and oil refining.

2.Experimental Methodology

The specimens used in the FSW investigations were made from SA516 Gr.70 N steel plates that were purchased on the open market and cut to 80 mm × 50 mm × 12 mm in size. The FSWM30NC machine was used to join two of these steel plates, as shown in Figure 1. To avoid any separation at the joint surfaces, the plates were placed adjacent to one another and firmly secured. The process created by TWI, as detailed in the Thomas et al. patent, served as the foundation for the FSW method used. Following the Taguchi DOE, this FSW technique involved manipulating three main variables: the tool's tilt angle with respect to the workpiece surface, the tool's rotational speed, the feed rate (tool movement speed), and the pin tool's length. The following section will go into more detail about these factors.

The carbon steel plates were welded in a direction parallel to the joint line. The material around the rotating pin was stirred and mixed by the tool's rotation, and the welding process was completed when the tool's linear motion transferred the stirred material from the front to the back of the pin. The tool's rotation with respect to the joint line determined the advancing and retreating sides of the welded plates. Because of its tilt to the trailing side, the tool's shoulder was able to hold onto the material that had been stirred by the threaded pin while transferring it from the front to the back of the pin with ease. The height (length) of the pin was related to its depth of insertion into the workpiece, and the depth of insertion determined the contact area between the workpiece surface and the tool shoulder. As a result,

the welded plates may have developed localized thinning, surface grooves, inner channels, or excess flash.

Additionally, PWHT was carried out in compliance with the rules outlined in ASME Section VIII Div. 1. The welded joints mechanical qualities and integrity were guaranteed by the PWHT process, which involved precisely regulated heating and cooling rates. This improved the joints performance and dependability.



Figure 1. FSW process.

3.Materials and Methods

The focus of this study is low carbon steel, specifically ASME SA516 Grade 70 N, commonly known as pressure vessel steel. Tables 1 and 2 provide detailed information about the material's composition and mechanical properties. The material was supplied as normalized steel plates. We used the test certificates supplied by the manufacturing company to thoroughly assess the chemical makeup of the steel plates and the related tool material. These certifications include vital information that demonstrates the precision of the material's requirements and guarantees conformity to industry norms, both of which are necessary for its use in high pressure settings.

Table 1 Parent material mechanical properties

Material	**SA 516 Gr.70N**	
Properties	Required	Actual
Yield strength (Mpa)	220(min)	243

Tensile Strength (Mpa)	415-550	489
Elongation (%)	27(min)	32

Table 2 Parent material chemical compositions

Comp. (%)	**Required**	**Actual**
C	0.28(max)	0.14
Mn	0.79-1.30	1.26
Si	0.13-0.45	0.32
P	0.035	0.004
S	0.035	0.0005
Cu	-	0.19
Ni	-	0.22
Cr	-	0.07
V	-	0.001
Ti	-	0.014
Al	-	0.024

4.Welding Process

The L9 orthogonal array design has been successfully used in executing the FSW process for studying the effects of the three most critical parameters on the mechanical characteristics of joints in low carbon steel. The parameters under investigation were tool diameter, welding speed, and tool rotation speed. The levels 1000, 1100, and 1200 rpm were examined for this variable, which has significance because it is said to affect the flow of material and bonding quality, because of the heat produced during welding. The three welding speeds 40, 55, and 70 mm/min each gave to heat input into the joint and hence to mechanical properties and microstructure of the weld. In addition, the sizes were evaluated at diameters of 4, 5, and 6 mm since the parameter also greatly affects how much material can be stirred and consequently shapes the weld and affects its strength. The L9 orthogonal array design made it possible to make a good assessment of all these parameters by using a systematic approach to modifying them, while considering their possible. Therefore, the quality of the welded joint may be fully understood owing to this strategy improving the reliability of the findings. Sample welding operation at 1000 rpms of tool rotation speed, 40 mm/min of welding speed, and a pin diameter of 4 mm is presented in Figure 2 as a reference amid changing the other parameters. Through this systematic study, it is hoped that optimal conditions will be determined by which the best mechanical properties are gained upon welding low carbon steel, which could have large implications for manufacturing processes. The ANSYS data for SA 516 shows that, as the tool's rotational speed rises, so does the temperature of the weldment; but the opposite is true when the welding speed increases. [37-38].

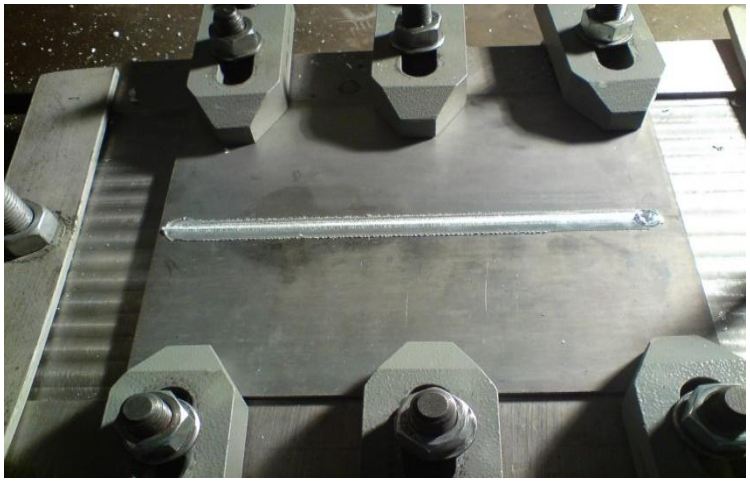


Figure 2. Sample 1 FSW

The L9 orthogonal array was used in this investigation to simplify the experimental protocol by examining a number of factors while reducing the overall number of experiments necessary. As shown in Table 3, it consists of nine different experimental runs that carefully balance three major parameters: tool diameter, welding speed, and rotation speed. The L9 design thus permits a balanced assessment of the interactions and effects of these parameters on the mechanical properties of low carbon steel joints, each being considered at three levels. Such an approach not only enhances the efficiency of the experimental procedure, but also allows one to optimize the knowledge gained from each run resulting in important findings at minimal expense in time and cost. Thus, the L9 orthogonal array is a potent means of refining welding conditions and the overall properties of the welded joints, thereby contributing meaningfully to the fields of materials engineering and manufacturing processes.

Table 3. Process Parameters.

S. No	Tool rotation Speed (rpm)	welding speed (mm/min)	Pin Diameter (mm)
FSW 1	1000	40	4
FSW 2	1000	55	5
FSW 3	1000	70	6
FSW 4	1100	40	5
FSW 5	1100	55	6
FSW 6	1100	70	4
FSW 7	1200	40	6
FSW 8	1200	55	4
FSW 9	1200	70	5

4.1 Post Weld Heat Treatment details

PWHT was carried out for low carbon steel FSW joints, in accordance with ASME Section VIII Division 1, to improve material strength, relieve residual stresses, and to acquire hardness within the specification ranges. The PWHT procedure was done in accordance with ASME Section VIII Division 1 requirements regarding UCS 56-1 through UCS 56-11, which publishes heating cycle data required for PWHT material specifications according to the P Number and group number of the material as mentioned in ASME Section IX.

The cycle parameters and requirements for this treatment were as follows: heating temperature from 610 to 630°C; holding time of 150 minutes to allow even temperature distribution and effective stress relief; heating rate of 85°C/h to minimize thermal shock; and cooling rate of 45°C/h in a controlled way to avoid further introduction of any new stresses in the material, as categorized in Table 4. The aim of this exhaustive PWHT procedure is to enhance the mechanical properties of the FSW joints so that they sufficiently meet the performance standard required for the applications for which they are intended.

Table 4 PWHT details

Sl.no	Description	Value
1	Temperature range	610-630°C
2	Soaking Period	150 Minutes
3	Heating rate	85°C/ Hr
4	Cooling rate	45°C/ Hr

4.2 Tensile test

In order to determine the mechanical property of the weld joints, tensile tests were performed on welded specimens following ASME Section IX and ASTM A370. Specimens were as welded as well as PWHT processed. The specimens were prepared to ASTM A370 dimension and gauge length standards to ensure trueness in measurement of yield strength, ultimate tensile strength, elongation, and area reduction. The as welded specimens were used for initial tensile test for assessing mechanical integrity. Thereafter, PWHT was carried out on a fraction of welded samples in order to relieve residual stress and improve ductility. Table 5 tabulates the PWHT effect on weld quality, as appreciated from the difference in mechanical properties determined from subsequent tensile testing of the PWHT samples. This test shows the measure of properties associated with the performance of welded joints, and consequently would help understand and improve welding procedures as per adopted industry standards.

Table 5. Tensile test (Before &after PWHT)

S.No	Tensile test (Before PWHT) MPa	Tensile test (After PWHT) MPa	Hardness test (Before PWHT) HV	Hardness test (After PWHT) HV	Impact test (Before PWHT) J	Impact test (After PWHT) J
FSW 1	520	500	186	170	76	69
FSW 2	487	482	174	172	78	70
FSW 3	478	461	166	159	81	71
FSW 4	540	523	188	179	82	75
FSW 5	496	485	174	164	76	70
FSW 6	489	470	177	162	76	71
FSW 7	488	470	173	166	78	72
FSW 8	479	463	168	159	80	73
FSW 9	535	515	187	173	79	73

Tensile strength measurement shows variations in samples before and after PWHT. Before PWHT, the tensile strength values are in the range of 478 MPa and 540 MPa with an average strength of about 496 MPa, indicating a fairly good performance overall by the samples. On the contrary, all specimens lost their tensile strength after PWHT, with a decrease in tensile strength values of between 461 MPa to 523 Mpa is represented in Figure 3. This may be due to the stress relief and microstructure alteration caused by heat treatment, emphasizing the effect of PWHT on the mechanical integrity of welded joints

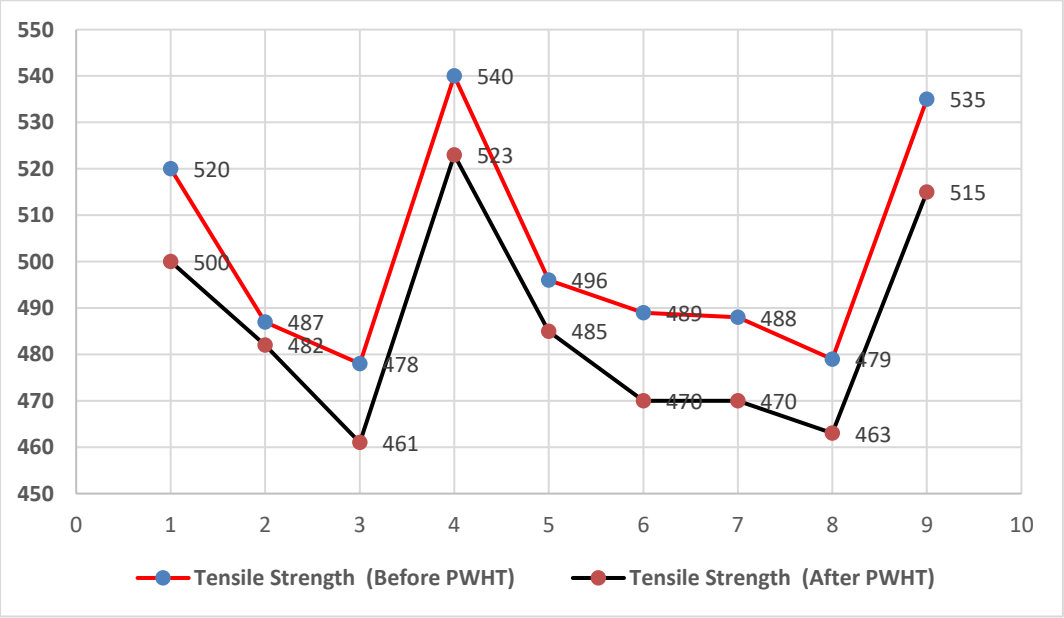


Figure 3. Tensile Strength (Before &After PWHT)

4.3 Hardness test

The hardness tests were done on the welded samples according to ASME Section V and ASTM E384-16 to evaluate the mechanical properties in the parent metal, heat affected zone (HAZ), and weld metal. All nine specimens were hardened through a hardness tester as welded and after PWHT. The specimens were prepared based on ASTM specifications to achieve appropriate sizes for testing. The hardness values of each area of interest were noted, with results carefully calculated and averaged before being condensed into a table of easy comparison. This thorough evaluation of hardness over various weld regions contributes significantly towards a better understanding of the mechanical behaviour of welded joints and provides key insights into the effects of the welding process and subsequent heat treatments.

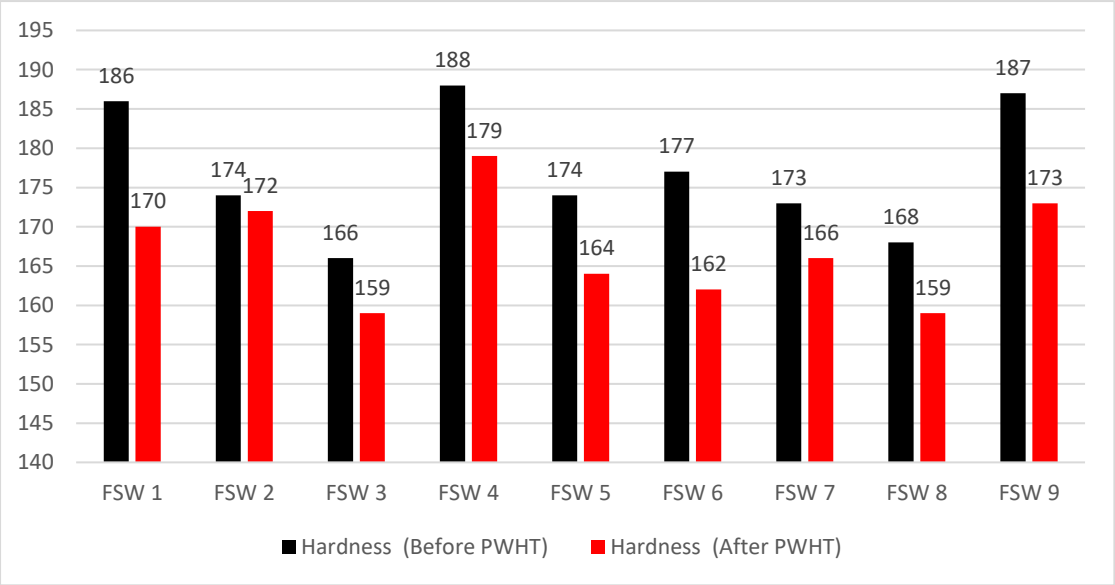


Figure 4. Hardness Test (Before &After PWHT)

Furthermore, hardness testing of the FSW specimens strengthens observation of PWHT's effect on the weld mechanical properties. Hardness values prior to PWHT, which were said to have represented the welded materials strength characteristics, ranged from 166 HV to 188 HV. However, PWHT exhibited a general decrease in hardness, with final values ranging from 159 HV to 179 HV as shown in Figure 4. This reduction implies that there must be a compromise between strength and ductility in PWHT welded joints and indicates the possible formation of a ductile microstructure as a result of the softening effects due to stress relief of the heat treatments that decrease hardness.

4.4 Impact test

In term of standards and acceptance criteria, the impact toughness of welded joints shall be assessed according to recognized code specifications such as ASME Section VIII Division 1, ASME Section IX, and ASTM A516/A516M. For example, for materials such as SA-516 Grade 70, impact tests are generally performed at -20°C (-4°F) or 0°F in order to represent service conditions at low temperature. The acceptance criteria normally stipulate a minimum average impact energy of 20 Joules (roughly 15 ft-lb), and that no individual specimen shall have an impact energy of less than 16 Joules (approximately 12 ft-lb). The mentioned criteria guarantee that welded joints are adequately tough in resisting service environments, and if at

low temperature, brittle fracture might be a hazard. Welds shall be qualified for structural applications only if the impact test results meet or pass the present acceptance criteria; otherwise, the process may have to be modified or the welds may have to be subjected to additional heat treatment to improve toughness.

Prior to PWHT, all FSW joints had good toughness with impact energies ranging from 76 to 82 Joules. Among them, FSW 4 had an impact energy of 82 Joules, which indicates the best toughness. Impact toughness values of the welds are well above the minimum requirements normally prescribed for structural steels such as ASTM A516 Grade 70, which are normally impact tested at -20°C (or 0°F). After PWHT, all samples saw a decrease in impact test values, with the highest reading of 75 Joules being recorded in FSW 4. The decrease in the value shows the microstructural refinement and residual stress relief; hence, further improvement of weld mechanical properties is achieved.

5. Results and Discussion

5.1 Tensile Strength Analysis

With variations in tool rotation speed, welding speed, and pin diameter, tensile strength exhibited a nonlinear trend. Tensile strength was comparatively low at lower tool rotation speeds (1000 rpm), and it continued to decline after PWHT. Tensile strength increased to a maximum of 540 N prior to PWHT when the rotation speed was raised to 1100 rpm (FSW 4: 1100 rpm, 40 mm/min, 5 mm pin diameter). The tensile strength, however, generally declined somewhat at 1200 rpm, suggesting that too much heat input at high rotation speeds causes softening and reduced joint strength. According to the general trend, very high or very low tool rotation speeds weaken the tool, while moderate speeds produce the best tensile properties.

Tensile strength clearly decreased with increasing welding speed. The highest tensile strength values were recorded at 40 mm/min, as in FSW 4 (540 N before PWHT, 523 N after PWHT). Tensile strength values decreased somewhat as welding speed increased to 55 mm/min; the lowest tensile strength was measured at 70 mm/min (FSW 3: 478 N before PWHT, 461 N after PWHT). This suggests that inadequate heat input from higher welding speeds results in inadequate material mixing and decreased tensile strength. The pattern demonstrates how better material flow and joint consolidation at lower welding speeds produce stronger welds.

There was a trend in the influence of pin diameter as well. Tensile strength was typically lower for smaller pin diameters (4 mm), while the highest values were obtained for pin diameters of 5 mm. FSW 4 (1100 rpm, 40 mm/min, 5 mm pin diameter) and FSW 9 (1200 rpm, 70 mm/min, 5 mm pin diameter) showed the best tensile strength, indicating that a 5 mm pin diameter improves mechanical interlocking. Tensile strength, however, dropped as the pin diameter rose to 6 mm, most likely as a result of excessive material stirring and potential defect formation. According to the findings, pin diameters that are too small or too

large have a negative impact on strength, while moderate diameters (5 mm) offer the best tensile characteristics.

5.2 Hardness Strength Analysis

Because of the tempering effect, which lowers internal stresses and softens the material, the hardness of the FSW joints showed a declining trend following PWHT. The maximum hardness was 188 HV prior to PWHT (FSW 4: 1100 rpm, 40 mm/min, 5 mm pin diameter), and it dropped to 179 HV following PWHT. Likewise, prior to PWHT, the lowest hardness was 166 HV (FSW 3: 1000 rpm, 70 mm/min, 6 mm pin diameter), and following PWHT, it further decreased to 159 HV. This implies that whereas lower hardness values exhibit a smaller reduction, higher initial hardness values are more impacted by PWHT.

Hardness was found to be significantly impacted by tool rotation speed. Prior to PWHT, hardness values at 1000 rpm ranged from 166 to 186 HV; following heat treatment, they further decreased. At 1100 rpm, the hardness rose to its maximum value of 188 HV, suggesting that moderate rotation speeds produce the best heat input and produce a fine grained structure. Hardness, however, dropped once more at 1200 rpm, indicating that too much heat input causes the material to soften. The trend demonstrates that the best hardness values both before and after PWHT are obtained at 1100 rpm.

Hardness trends were also impacted by welding speed. Hardness values were higher at lower welding speeds (40 mm/min), suggesting improved material refinement and bonding. Hardness, however, decreased with increasing welding speed to 70 mm/min; FSW 3 had the lowest values (166 HV before PWHT, 159 HV after PWHT). This implies that greater welding speeds result in lower hardness values by reducing heat input and plastic deformation. The relationship between pin diameter and hardness was comparable to that of tensile strength. As demonstrated by FSW 4 (188 HV before PWHT, 179 HV after PWHT) and FSW 9 (187 HV before PWHT, 173 HV after PWHT), the highest hardness values were obtained with a 5 mm pin diameter. Conversely, lower hardness values were observed for pin diameters of 4 and 6 mm, suggesting that an ideal pin diameter of 5 mm helps to improve hardness retention even after PWHT.

5.3 Impact Test analysis

The impact testing gave results of FSW joints made with assorted sets of process parameters whose influence on the mechanical performance and microstructures of the welded joints could have been studied. Impact energies were measured from 76 Joules to a maximum of 82 Joules, suggesting that the welds have good toughness and energy absorption capacity. In particular, the weld carried out at a speed of 1100 rpm for the tool rotation, 40 mm/min for the welding speed, and a pin diameter of 5 mm, referred to as FSW 4, exhibited the best impact energy of 82 Joules, showing the best toughness; hence, these specific parameters seem favorable for microstructural refinement and defect free weld formation.

Further data analysis shows that raising the tool rotation speed from 1000 rpm to 1200 rpm tends to improve the impact toughness of the welds, particularly when paired with

moderate welding speeds of 40 to 55 mm/min. Better material mixing, finer grain structures, and less porosity or flaws within the weld zone are all facilitated by the increased heat input and mechanical stirring that come with greater rotational speeds. Improved energy absorption during impact testing is directly a result of these microstructural improvements. On the other hand, welds with somewhat lower impact energies are typically produced by lower rotating speeds or extremely high welding rates. This could be because of inadequate heat input or mixing, which results in finer microstructures or residual stresses that compromise toughness.

Although it also affects impact performance, the difference in pin diameter, which ranges from 4 to 6 mm, seems to be less important than the combination of welding and rotating speeds. Greater stirring action is typically encouraged by larger pin sizes; nevertheless, the interaction of process variables, not just pin size, largely determines the best impact toughness outcomes. FSW 8, for instance, obtained an impact energy of 80 Joules, which is near the maximum, with a welding speed of 55 mm/min, a rotation speed of 1200 rpm, and a 4 mm pin. This further supports the idea that higher mechanical qualities are produced by the optimal combination of parameters.

The impact values decreased across all samples after PWHT, with the highest impact value being 75 Joules, indicating microstructural strengthening through processes like grain growth control and residual stress relief. This increase in impact test indicates that PWHT not only improves the microstructural stability but also increases the overall toughness and load bearing capacity of the welds. PWHT has a significant impact on the microstructure and mechanical properties of the welds.

5.4 Microstructure analysis

As is typical of low carbon steels, the base metal has a traditional ferrite pearlite microstructure. Because of its soft and ductile characteristics, ferrite represented by the lighter phase in this microstructure is appropriate for applications requiring high formability and resilience. The alternating layers of cementite and ferrite form the darker phase, pearlite, which adds to the materials overall strength and hardness as shown in Figure 5(a). Because the base metal is located away from the heat produced during the FSW process, its grain structure is stable and mainly unaffected. This guarantees that the base metals mechanical qualities are maintained, giving the welded joint a strong base.

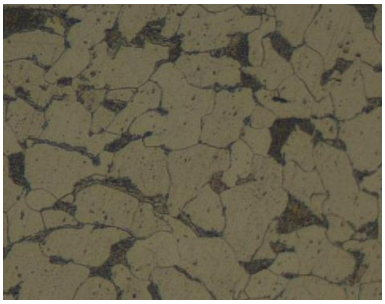
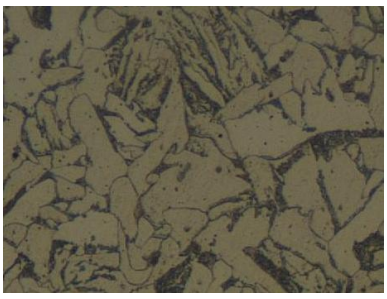
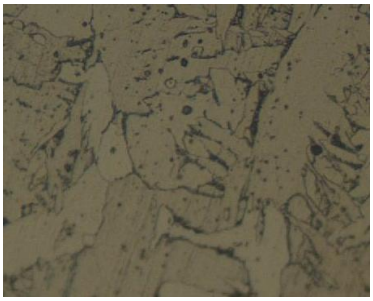
		
Figure 5 (a) Base metal	**Figure 5 (b) HAZ**	**Figure 5 (c) Stir zone**

Figure 5. Microstructure of FSW welded carbon steel Before PWHT

The welding process thermal cycles caused notable microstructure changes in the HAZ. Grain coarsening results from localized heating in the HAZ, as the ferrite grains enlarge due to the high temperatures. Some pearlite may dissolve as a result, reducing its strength contribution as shown in Figure 5(b). It is possible for bainitic or martensitic structures, which are generally harder but more brittle than the parent ferrite pearlite structure, to form when the heat input is exceptionally high. Strength and toughness must be carefully balanced during the welding process because this change in microstructural properties may affect the joints mechanical performance.

The microstructure of the stir zone differs significantly from that of the base metal and HAZ due to its strong plastic deformation and dynamic recrystallization during the FSW process. The microstructure in this case is made up of fine grained, equiaxed ferrite, which, thanks to its refined grain structure shown in Figure 5(c), increases both toughness and strength. Dendritic structures, which are frequently observed in fusion welds, do not form in the stir zone of solid state welding processes due to the lack of melting, in contrast to conventional fusion welding techniques. The thermo mechanically affected zone (TMAZ), which surrounds the stir zone, exhibits elongated and deformed grains as a result of the high temperatures and mechanical working. This unique microstructural combination contributes to the overall performance of the weld, offering a blend of strength and ductility essential for many engineering applications.

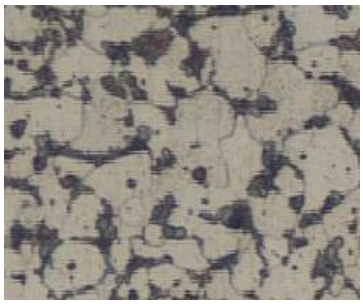
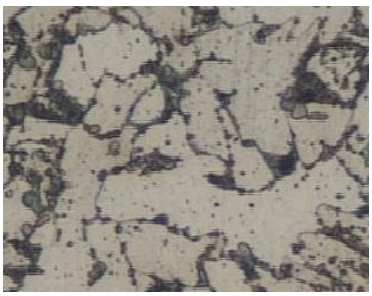
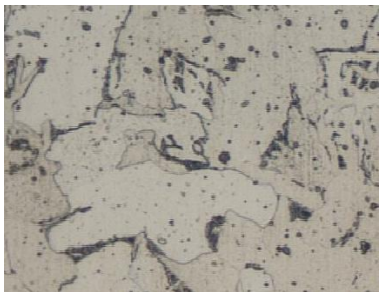
		
Figure 6 (a) Base metal	**Figure 6 (b) HAZ**	**Figure 6 (c) Stir zone**

Fig 6. Microstructure of FSW welded carbon steel After PWHT

The microstructural changes in base metal following PWHT are only minor as the metal has been subjected to prior heat during welding; one of these changes being a slight increase in grain size. The ferrite pearlite microstructure, which inherits some intrinsic mechanical properties considered essential for the performance of the material, prevails in Figure 6(a). Since ferrite is continuously present, the base metal is ductile and malleable, which are some of the characteristics desired in applications requiring high resilience and formability. Thus, this stability adds to the importance of the base metal concerning the entire welded assembly and contributes to the structural integrity of the component.

PWHT is necessary to modify the coarse grained microstructure produced due to welding in the HAZ. The higher temperature at that region gives rise to harder martensitic or bainitic structures, possibly leading to a loss of ductility. However, after PWHT, these might revert back and temper to form pearlite and softer ferrite, which can greatly enhance the ductility within the HAZ, as shown in Figure 6(b). This change drastically lowers the possibility of the material being brittle fractured and cracking under stress, thus increasing the entire reliability of the material while in use. The benefits of this microstructural modification become more icon when under dynamic loading conditions on the welded component.

The initially fine grained ferrite structure represented in Figure 6(c) is then stabilized and stress relieved through PWHT in the stir zone. In addition, it maintains the fine grain morphology, which adds it to the toughness of weld metal, and improves microstructural stability. The reduction of residual stresses, which usually persist after the welding process, is most interesting since it increases the fatigue resistance and the welded joints strength under cyclic loading. In short, PWHT encourages the reduction in hardness while ductile and toughness enhancement is developed in the weld, making it more appropriate for structural applications requiring high levels of fatigue strength and impact resistance. All of this improvement is very significant in illustrating the importance of PWHT to the assurance of reliability and performance over time of welded low carbon steel components.

5.5 Phase/ volume fraction analysis of weld metal

Phase quantification of SA-516 Gr.70 after friction stir welding shows the microstructure comprising 49.16% pearlite and 50.84% ferrite shown in Figure 7 (a). PWHT causes a change, with the pearlite reducing to 45.43%, while the ferrite content increases to 54.57% shown in Figure 7 (b). Fine and dense structures are present before PWHT, whereas coarsened grains and phase boundaries are seen in the post PWHT microstructures. This is due to changes caused by diffusional and tempering effects of PWHT, as the pearlite undergoes spheroidization while ferrite grains grow: this is primarily responsible for the transformation in the mechanical properties.

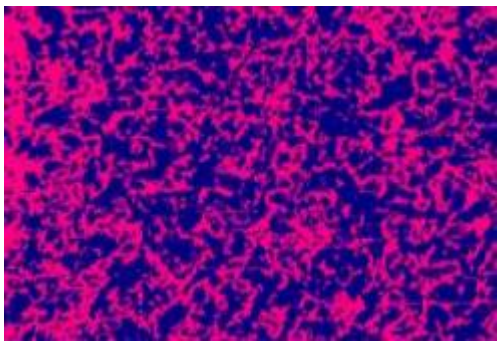


Figure 7 (a) Before PWHT

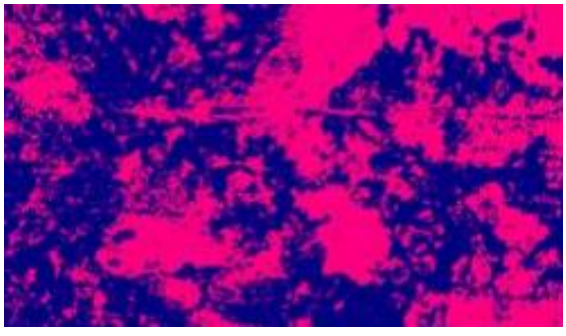


Figure 7 (b) After PWHT

Fig 7. Phase/ volume fraction FSW (Before and After PWHT)

Due to the microstructural change, the average tensile strength drops slightly, generally from 495 MPa before PWHT to 481 Mpa. This is basically because of the reduction in pearlite that normally strengthens the material through its cementite lamellae. Conversely, impact toughness improves at room temperature from 78 J to 71 J. This change in ductility and the resistance to brittle fracture resulting from increased ferrite content and the stress relief are amongst the desired features in pressure-retaining applications.

The hardness is noticeably compromised in PWHT as the values drop from about 176 HV for the as-welded condition to roughly 165 HV after PWHT. These changes are caused by coarsening of the microstructure and partial decomposition of pearlite, which lessen resistance to localized plastic deformation. The decrease in hardness obtained serves as an indication of stress relief and the softening effect of PWHT. Strength is reduced somewhat, but the greatly enhanced ductility and toughness allow for improved long-term service, especially of welded joints under varying thermal or mechanical loads.

6.Conclusion

Research on friction stir welded low carbon steel and its PWHT effect has illustrated the principles behind the influence of welding speed, pin diameter, and tool rotation speed on hardness and tensile strength. The results reveal that maximum tensile strength before and after PWHT results from a moderate tool rotation speed (1100 rpm), low welding speed (40 mm/min), and ideal pin diameter (5 mm). Increased speed of the tool rotation (1200 rpm) and excess welding speed (70 mm/min) would lead to the decrease of mechanical properties due to high heat input or insufficient material consolidation.

Tensile strength began to decline after the PWHT. Just before PWHT, it had reached a maximum value of 540 N (FSW 4: 1100 rpm, 40 mm/min, 5 mm pin diameter); it later dropped to 523 N post PWHT. Microstructural softening and stress relaxation lead to this decrease. Hardness tests show that the values also dropped after PWHT, with highest initial hardness of 188 HV dropping to 179 HV post PWHT. Impact tests show that the values also dropped after PWHT, with highest impact value of 82 Joules dropping to 75 Joules post PWHT. Therefore, microstructural changes caused by PWHT on SA 516 Gr.70, i.e., greater volume of ferrite and spheroidized pearlite slightly reduce tensile strength and hardness but extremely improve impact toughness and ductility. These transformations, with diffusion and tempering in control, are effective in balancing strength with toughness and hence overall performance and reliability of welded pressure components.

The same ideal process parameters were also proposed by the L9 orthogonal array design of experiments, supporting the finding that the best mechanical performance for FSW welding with or without PWHT is provided by a tool rotation speed of 1100 rpm, a welding speed of 40 mm/min, and a pin diameter of 5 mm. These results are essential for balancing strength, hardness, impact test and weld integrity for industrial use when optimizing FSW parameters in low carbon steel applications.

Acknowledgements: Not Applicable

Authors Contributions: MFS and MNI collaboratively developed the conceptual framework and research scope, designing the methodology and experimental procedures. MFS conducted the experimental investigations, including performing friction stir welding, applying PWHT, and collecting data on mechanical properties and microstructural changes. Both authors sourced materials, prepared welding setups, and carried out testing such as hardness measurements, tensile tests, and microstructural analyses. MFS was responsible for drafting the original manuscript, while both MFS and MNI contributed to editing and refining the final version. MNI provided research supervision, guiding the overall process, ensuring adherence to protocols, and offering scientific insights. Additionally, MNI managed project administration, coordinating tasks, overseeing progress, and facilitating effective communication to ensure the successful completion of the study.

Funding

This research did not receive any particular funding from public, commercial, or non profit organizations

Availability of data and materials

All presented data are available upon request

Conflicts of interest

The authors declare that they have no conflicts of interest regarding the publication of this paper.

References

1. W.M. Thomas, E.D. Nicholas, J.C. Needham, M.G. Murch, P. Temple-Smith, C.J. Dawes, International Patent Application No PCT/GB92/02203.
2. Threadgill, P. L., A. J. Leonard, H. R. Shercliff, and P. J. Withers. "Friction stir welding of aluminium alloys." International Materials Reviews 54, no. 2 (2009): 49-93. https://doi.org/10.1179/174328009X411136
3. Ahmed, Mohamed MZ, Mohamed M. El-Sayed Seleman, Dariusz Fydrych, and Gürel Çam. "Friction stir welding of aluminum in the aerospace industry: the current progress and state-of-the-art review." Materials 16, no. 8 (2023): 2971. https://doi.org/10.3390/ma16082971
4. Zamrudi, Firdausi H., and Asep R. Setiawan. "Effect of friction stir welding parameters on corrosion behaviour of aluminium alloys: an overview." Corrosion Engineering, Science and Technology 57, no. 7 (2022): 696-707. https://doi.org/10.1080/1478422X.2022.2116185
5. Birol, Y., and S. Kasman. "Effect of welding parameters on microstructure and mechanical properties of friction stir welded EN AW 5083 H111 plates." Materials Science and Technology 29, no. 11 (2013): 1354-1362.https://doi.org/10.1179/1743284713Y.0000000280
6. Sivakumar, C. K., Y. Robinson, P. Prema, S. Joe Patrick Gnanaraj, and M. Appadurai. "Mechanical characteristics of aluminium alloy joints produced by friction stir welding." Materials Today: Proceedings 62 (2022): 5620-5624. https://doi.org/10.1016/j.matpr.2022.04.831
7. Trojovský, Pavel, Vigneswaran Dhasarathan, and Sampath Boopathi. "Experimental investigations on cryogenic friction-stir welding of similar ZE42 magnesium alloys." Alexandria Engineering Journal 66 (2023): 1-14. https://doi.org/10.1016/j.aej.2022.12.007

8. Khalid, Eisha, Vasanth C. Shunmugasamy, and Bilal Mansoor. "Microstructure and tensile behavior of a Bobbin friction stir welded magnesium alloy." Materials Science and Engineering: A 840 (2022): 142861. https://doi.org/10.1016/j.msea.2022.142861
9. Chiuzuli, Fernanda Rocha, Bruna Fernanda Batistao, Luciano Andrei Bergmann, Nelson Guedes de Alcantara, Jorge Fernandez dos Santos, Benjamin Klusemann, and Piter Gargarella. "Effect of the gap width in AZ31 magnesium alloy joints obtained by friction stir welding." Journal of Materials Research and Technology 15 (2021): 5297-5306. https://doi.org/10.1016/j.jmrt.2021.10.115
10. Zhou, Ziru, Songlin Zheng, Jiahuan Chen, Ting Zhang, Zhen He, and Yuxin Wang. "Corrosion and protection of friction stir welding of magnesium alloy." Anti-Corrosion Methods and Materials 71, no. 1 (2024): 47-54. https://doi.org/10.1108/ACMM-07-2023-2853
11. Gao, Shikang, Hongyun Zhao, Gaohui Li, Guangda Sun, Li Zhou, and Yaobang Zhao. "Strengthening mechanism and corrosion behavior of friction stir welded LAZ933 magnesium-lithium alloy." Journal of Magnesium and Alloys (2023). https://doi.org/10.1016/j.jma.2023.03.003
12. Wang, Y. D., P. Xue, F. C. Liu, L. H. Wu, H. Zhang, Z. Zhang, D. R. Ni, B. L. Xiao, and Z. Y. Ma. "Influence of processing innovations on joint strength improvements in friction stir welded high strength copper alloys." Materials Science and Engineering: A 872 (2023): 144983. https://doi.org/10.1016/j.msea.2023.144983
13. Thapliyal, Shivraman, and Akshansh Mishra. "Machine learning classification-based approach for mechanical properties of friction stir welding of copper." Manufacturing Letters 29 (2021): 52-55. https://doi.org/10.1016/j.mfglet.2021.05.010
14. Sun, Yumeng, Wenbiao Gong, Rui Zhu, Yupeng Li, and Shicheng Sun. "Research progress and prospect of friction stir welding of copper and copper alloys." Metallurgical Research & Technology 120, no. 3 (2023): 309. https://doi.org/10.1051/metal/2023011
15. Fayas, Mohamed, Dinu Thekkuden, Abdel Hamid Ismail Mourad, Abdullah Syed, Khalid Alsayed, Yassir Amri, and Mohammad Qahtani. "Combined Gas Tungsten Arc Welding and Shielded Metal Arc Welding Processes for joining tube to tubesheet in Shell and Tube Heat Exchangers." Journal of Pressure Vessel Technology (2024): 1-11. https://doi.org/10.1115/1.4065519
16. Mohamed Fayas Saffiudeen and Inamdar, Mohammad Nizamuddin, "Review on Friction Stir Welding of Carbon Steel." Eur. Chem. Bull. 12, no. Special Issue 1, Part-B (2023): 3867-3877. https://doi.org/10.31838/ecb/2023.12.s1-B.389.
17. Thekkuden, Dinu Thomas, Abdel-Hamid Ismail Mourad, Tholkappiyan Ramachandran, Abdel-Hakim Bouzid, Ravi Kumar, and Ahmed Alzamly. "Combined effect of tungsten inert gas welding and roller expansion processes on mechanical and metallurgical characteristics of heat exchanger tube-to-tubesheet joints." journal of materials research and technology 21 (2022): 4724-4744. https://doi.org/10.1016/j.jmrt.2022.11.043
18. Saffiudeen, Mohamed Fayas, Fasil T. Mohammed, and Abdullah Syed. "Comparative study of tube to tubesheet welding qualification on heat exchanger." Journal of Engineering and Applied Science 69, no. 1 (2022): 57.https://doi.org/10.1186/s44147-022-00099-z
19. Thekkuden, Dinu Thomas, Abdel-Hamid Ismail Mourad, and Abdel-Hakim Bouzid. "Failures and leak inspection techniques of tube-to-tubesheet joints: A review." Engineering Failure Analysis 130 (2021): 105798. https://doi.org/10.1016/j.engfailanal.2021.105798
20. Saffiudeen, Mohamed Fayas, Fasil T. Mohammed, and Abdullah Syed. "A case study on procedure standardization of heat exchanger retubing in KSA oil and gas industries." Journal of Failure Analysis and Prevention 20, no. 5 (2020): 1451-1455. https://doi.org/10.1007/s11668-020-00965-z
21. Bassey, Michael, Umoh Offiong, and Aniekan Ikpe. "Finite element simulation for thermo-mechanical transient behavior of mild steel plate agglutinated by gas tungsten arc welding (GTAW) technique." Journal of materials engineering, structures and computation 2, no. 3 (2023). https://doi.org/10.5281/zenodo.8306756

22. Senthilkumar, S., S. Manivannan, R. Venkatesh, and M. Karthikeyan. "Influence of heat input on the mechanical characteristics, corrosion and microstructure of ASTM A36 steel welded by GTAW technique." Heliyon 9, no. 9 (2023). https://doi.org/10.1016/j.heliyon.2023.e19708
23. Manh, Ngo Huu, Han Le Duy, Murata Akihisa, Trinh Quang Ngoc, and Bharat Gandham. "Development of a novel GTAW process for joining ultra-thin metal sheets." Journal of Manufacturing Processes 80 (2022): 683-691. https://doi.org/10.1016/j.jmapro.2022.06.043
24. Deepak, J. R., J. Jeya Jeevahan, D. Ramachandran, SV Sai Suhas, and PV Praneethkumar Reddy. "XRD investigation of GTAW, GMAW, LBW and AGTAW Corten A588 grade steel weldments." Materials Today: Proceedings 47 (2021): 4844-4851. https://doi.org/10.1016/j.matpr.2021.06.081
25. Mushthofa, Malik, Fakhri Pratama Nurfauzi, and Astriana Hardawati. "Investigation of effective section reduction in low carbon steel during SMAW welding." Teknisia 28, no. 2 (2023): 79-89. https://doi.org/10.20885/teknisia.vol28.iss2.art2
26. Kai, Lester Chin Zen, Sung Aun Naa, and Edwin Jong Nyon Tchan. "A Study of Weld Seams on Low Carbon Steel ABS Grade a Marine Plates Using SMAW Process." Journal of Sustainable Manufacturing in Transportation 3, no. 1 (2023): 9-20. https://publisher.uthm.edu.my/ojs/index.php/jsmt/article/view/14198.
27. Ranjan, Rajeev, Sanjay Kumar Jha, Pradeep Kumar Mouria, and Subhash Mishra. "Investigation of post weld heat treatment on mechanical properties of low frequency vibration assisted SMAW mild steel welded joints." International Journal on Interactive Design and Manufacturing (IJIDeM) 18, no. 8 (2024): 5489-5500. https://doi.org/10.1007/s12008-024-01793-3
28. Saffiudeen, Mohamed Fayas, Vasanth Swaminathan, Fasil T. Mohammed, Abdullah Syed, Yassir A. Alamri, and Mohammad N. Al Qahtani. "Experimental Investigation on Stainless-Steel Weld Overlay on Carbon Steel Plates Using Different Electrodes." Arabian Journal for Science and Engineering (2024): 1-11.https://doi.org/10.1007/s13369-024-09559-5
29. Tukahirwa, Gilbert, and Catherine Wandera. 2023. 'Influence of Process Parameters in Gas-Metal Arc Welding (GMAW) of Carbon Steels'. Welding - Materials, Fabrication Processes, and Industry 5.0. IntechOpen. doi:10.5772/intechopen.1002730.
30. Grzybowski, Igor Felipe, Renan Rakoski Zientarski, Alexandre Aparecido Buenos, and Auteliano Antunes dos Santos Junior. "Residual stresses in weld bead of low carbon steel plates welded by GMAW using LCR waves." Journal of the Brazilian Society of Mechanical Sciences and Engineering 44, no. 7 (2022): 290. https://doi.org/10.1007/s40430-022-03587-8
31. Ramarao, M., M. Francis Luther King, A. Sivakumar, V. Manikandan, M. Vijayakumar, and Ram Subbiah. "Optimizing GMAW parameters to achieve high impact strength of the dissimilar weld joints using Taguchi approach." Materials Today: Proceedings 50 (2022): 861-866. https://doi.org/10.1016/j.matpr.2021.06.137
32. Ungethüm, T., P. Schilling, E. Spaniol, and U. Füssel. "GMAW hot-wire process with indirect resistive heating of the auxiliary wire." Welding in the World 67, no. 8 (2023): 2031-2038. https://doi.org/10.1007/s40194-023-01529-z
33. Neumann, M., A. Haelsig, K. Hoefer, and J. Hensel. "Thick-wire GMAW for fusion welding of high-strength steels." Proceedings of the Institution of Mechanical Engineers, Part L: Journal of Materials: Design and Applications 238, no. 12 (2024): 2487-2499. https://doi.org/10.1177/14644207241283273
34. Aswal, Vinod Kumar, Jinesh Kumar Jain, and Pankaj Sonia. "Review on the behavior of various parameters on heat distribution in the SAW process." Materials Today: Proceedings 47 (2021): 6734-6739. https://doi.org/10.1016/j.matpr.2021.05.123
35. Shrimali, Ritesh, Manoj Kumar, Sunil Pandey, Vikram Sharma, Lokesh Kaushik, and Karan Singh. "A robust Taguchi combined AHP approach for optimizing AISI 1023 low carbon steel weldments in the SAW process." International Journal on Interactive Design and Manufacturing (IJIDeM) 17, no. 4 (2023): 1959-1977. https://doi.org/10.1007/s12008-023-01307-7
36. Sabry, Ibrahim, Ahmed M. El-Kassas, Abdel-Hamid I. Mourad, Dinu Thomas Thekkuden, and Jaber Abu Qudeiri. "Friction stir welding of T-joints: experimental and statistical analysis." Journal of Manufacturing and Materials Processing 3, no. 2 (2019): 38. https://doi.org/10.3390/jmmp3020038

37. Saffiudeen MF, Inamdar MN. Thermal Analysis of Low Carbon Steel (SA516 Gr. 70) Welding Through APDL. NanoWorld J9(S3) 2023: S629-S632. https://doi.org/10.17756/nwj.2023-s3-115

38. Cîndea, Lenuţa, Cornel Haţiegan, Nicolina Pop, Romeo Negrea, Eugen Răduca, Gilbert-Rainer Gillich, Moşteanu Dănuţ, and Marian-Dumitru Nedeloni. "The influence of thermal field in the electric arc welding of X60 carbon steel components in the CO2 environment." Applied Thermal Engineering 103 (2016): 1164-1175. https://doi.org/10.1016/j.applthermaleng.2016.05.004